Check for updates

Discovery of a novel rice-derived peptide with significant anti-gout potency†

Naixin Liu, ‡[a] Buliang Meng,‡[a] Lin Zeng,[d] Saige Yin,[a] Yan Hu,[a] Shanshan Li,[a] Yang Fu,[a] Xinping Zhang,[a] Chun Xie,[a] Longjun Shu,[c] Meifeng Yang,[a] Ying Wang*[c] and Xinwang Yang *[a,b]

As a metabolic disease, gout, which seriously affects the normal life of patients, has become increasingly common in modern society. However, the existing medicines cannot completely meet the clinical needs. In the current study, a novel short peptide (named rice-derived-peptide-2 (RDP2), AAAAGAMPK-NH2, 785.97 Da) was isolated and identified from water extract of shelled *Oryza sativa* fruits, without toxic side effects but excellent stability. Our results indicated that RDP2 (the minimum effective concentration is 5 µg kg^{-1}) induced a significant reduction in serum uric acid levels in hyperuricemic mice *via* suppressing xanthine oxidase activity and urate transporter 1 expression, as well as alleviated renal damage through inhibiting the activation of NLRP3 inflammasome. In addition, RDP2 can also alleviate paw swelling and inflammatory reactions in mice after subcutaneous injection of monosodium urate crystals. As mentioned above, we obtained a novel peptide which could work through all stages of gout, not only reducing uric acid levels and renal damage in hyperuricemic mice, but also alleviating inflammatory responses associated with acute gout attack, and thus provided a new peptide molecular template for the development of anti-gout drugs.

Introduction

Gout is a crystal-related arthropathy caused by the deposition of monosodium urate (MSU) and is related to hyperuricemia (HUA) induced by purine metabolism disorder and decline in uric acid excretion.[1] HUA is the basis of gout and its associated complications. Continuous and uncontrolled HUA not only induces acute gout attack, leading to severe pain, but can also cause kidney disease.[2] Severe HUA may lead to joint damage, renal function impairment, long-term hyperlipidemia, hypertension, diabetes, arteriosclerosis, and coronary heart disease.[3] Therefore, controlling uric acid levels and reducing

[a]*Department of Anatomy and Histology & Embryology, Faculty of Basic Medical Science, Kunming Medical University, Kunming, Yunnan, 650500, China. E-mail: yangxinwanghp@163.com; Tel: +86 13577174345*

[b]*Yunnan Key Laboratory of Pharmacology for Natural Products, Kunming Medical University, Kunming, Yunnan, 650500, China*

[c]*Key Laboratory of Chemistry in Ethnic Medicine Resource, State Ethnic Affairs Commission & Ministry of Education, School of Ethno-Medicine and Ethno-Pharmacy, Yunnan Minzu University, Kunming, Yunnan, 650504, China. E-mail: wangying_814@163.com; Tel: +86 13577154345*

[d]*Public Technical Service Center, Kunming Institute of Zoology, Chinese Academy of Sciences, Kunming, Yunnan, 650223, China*

†Electronic supplementary information (ESI) available. See DOI: 10.1039/d0fo01774d

‡These authors contributed equally to this work.

or alleviating complications in treatment are important measures for gout patients.

Under normal circumstances, uric acid in the body can be balanced through diet, purine synthesis, and tissue catabolism.[4] When uric acid metabolism is unbalanced, drug treatment is considered one of the best ways to control uric acid levels, including drugs that inhibit key enzymes of uric acid synthesis (*e.g.*, xanthine oxidase, XOD) or uric acid reabsorption proteins (*e.g.*, urate transporter 1, URAT1).[5] It should be noted that HUA can only be treated effectively after symptoms appear, and thus the patient may not only need to anti-inflammation, but also reduce the internal uric acid.[6] At present, approved drugs include: colchicine, nonsteroidal anti-inflammatory drugs (NSAIDs), glucocorticoids, and IL-1β antagonists (for anti-inflammation and analgesia); allopurinol, febuxostat, oxipurinol, and topiroxostat (for inhibiting uric acid synthesis); probenecid, benzbromarone, lesinurad and sulfinpyrazone (for promoting uric acid excretion); and rasburicase (for decomposing uric acid).[1,6–9] However, most anti-gout drugs have side effects that are difficult to control. For example, NSAIDs can easily induce peptic ulcers; allopurinol can induce severe skin rash and allergic reactions; febuxostat can cause cardiovascular incidents; benzbromarone can show hepatotoxicity; and probenecid can cause increased uric acid crystals in the kidneys.[1,7–9] In addition, most drugs are only effective for treating one symptom, and thus patients may need to use

two or more drugs in combination. These combinations may lead to unpredictable drug interactions and adverse reactions, thereby limiting the clinical use of such drugs.[10] Therefore, multifunctional anti-gout drugs that can work across the entirety of gout disease remain to be discovered.

In the research and development of new drugs, peptide medicines are particularly worthy of attention. Compared with small molecule drugs, they have stronger selectivity, better effect and less side effects in less dosage.[11,12] Moreover, with the development of modern technology, the cost of peptide production has been greatly reduced. Therefore, the research and development of peptide drugs has been favored by many researchers, and some existing peptide drugs have had a considerable consumer market, such as exenatide, insulin, ACEI peptide and so on.[13–15] However, there are only a few reported active peptides against HUA and gout, suggesting the research of anti-gout and HUA peptide is still in its infancy. For example, the research of N. Liu *et al.*, D. Kubomura *et al.*, Y. Li *et al.*, Y. Ma *et al.* and I. Murota *et al.* reported anti-hyperuricemia peptides, and that of K. A. Zoghebi *et al.*, Izabela Galvao *et al.*, Vincent Vanheule *et al.* and W. M. Mackin *et al.* reported anti-inflammation peptides in the gout attack period.[4,11,12,16–24] Therefore, the peptides for anti-gout still have broad research prospects.

In this study, we identified a novel peptide (named rice-derived-peptide-2 (RDP2), AAAAGAMPK-NH2) from water extract of shelled *Oryza sativa* fruits, and the biological activities were then researched. The research was focused on the discovery and biological functions of new anti-gout candidate drugs. The research not only provided a novel candidate drug for the development of anti-gout and anti-hyperuricemic medicines, but also indicated that Yunnan *O. sativa* has the potential to become a healthy and nutritious food for people with high uric acid level.

Results

Collection and purification of RDP2 from shelled *O. sativa* fruits

Procedures were established to obtain the active peptide based on previous research.[16] First, a Sephadex G-50 gel filtration column was used to analyze the water extract of shelled *O. sativa* fruits. The sample indicated by an arrow in Fig. S1A† was collected (consistent with Fig. 1A in our previous research[16]). Secondly, the collected sample was further separated and purified by RP-HPLC (reverse phase-high performance liquid chromatography) (Fig. S1B,† corresponding to Fig. 1B in our previous research[16]). The sample showing a peak in Fig. S1B† indicated by the arrow was collected and purified using the same HPLC procedures as mentioned above to obtain the peak with an elution time of 17.8 min (arrow in Fig. S1C†). After this, the sample was analyzed by mass spectrometry.

As shown in Fig. 1A, a peptide triplet with a single isotope m/z of 786.477–808.466–824.445 was observed in the sample.

Further, tandem mass spectrometry was used to elucidate the sequence of the peptide triplet and confirmed the sequence of the sample ("AAAAGAPMK-NH2", *i.e.*, RDP2, Fig. 1B).

RDP2 showed no hemolytic activity or acute toxicity

To evaluate the safety of RDP2, its hemolytic activity and acute toxicity were tested. As shown in Tables S1 and S2,† RDP2 showed no hemolytic activity or acute toxicity.

RDP2 showed good stability under various conditions

To research the characteristics of RDP2, its stability under different conditions was first detected. As shown in Fig. 1C, after repeated freezing and thawing (eight times), the remaining content of RDP2 in the test solution was about 80%. After 20 d at 4 °C and 37 °C, RDP2 content remained at 95% and 90%, respectively. After 12 d at 60 °C, RDP2 content remained at about 80%.

The stability of RDP2 in plasma was tested. As shown in Fig. 1D, after incubation with plasma for 7 h (Table S3†), RDP2 was completely degraded, with a half-life of about 1.4 h (calculated with GraphPad Prism software).

RDP2 was mainly distributed in the liver and kidneys

To directly observe the distribution of RDP2 in mice after injection, FITC-RDP2 (RDP2 with fluorescein isothiocyanate isomer tag) was synthesized and mice were observed using a small animal *in vivo* imaging system. As shown in Fig. 2E, after intraperitoneal injection, the drug rapidly distributed to the entire intraperitoneal area. Front and back images of mice were taken. Results showed that 60 min after the injection of FITC-RDP2, the drug was mainly distributed in the abdominal cavity of the animals, particularly the liver and kidneys.

RDP2 lowered serum uric acid levels and alleviated renal damage in HUA mice

Anti-hyperuricemic activity of RDP2 was determined by measuring serum uric acid and creatinine levels in HUA mice. As shown in Fig. 2A, the serum uric acid level in HUA mice was about three times that in the control group ($P < 0.001$, Control *vs.* Model on day 7), indicating the abnormal elevation of serum uric acid in mice. The allopurinol (Allo, 10 mg kg^{-1}) and benzbromarone (Benz, 8 mg kg^{-1}) groups demonstrated significant decreases in serum uric acid levels ($P < 0.001$ *vs.* Model on day 7). The serum uric acid concentrations in the RDP2 groups (5, 10, and 100 μg kg^{-1}) were 45.7 ± 1.5, 37.1 ± 0.6, and 29.8 ± 0.6 mg L^{-1}, respectively, indicating that RDP2 induced a concentration-dependent reduction in serum uric acid levels.

The serum creatinine level in the model group increased significantly compared with that in the control group and the serum creatinine levels in the Allo and Benz groups were significantly lower than the levels in the model group ($P < 0.001$, Fig. 2B). The serum creatinine concentrations in the RDP2 groups (5, 10, and 100 μg kg^{-1}) were 103.5 ± 36.9, 95.1 ± 29.5, and 38.6 ± 9.5 μM, respectively. The treatment of RDP2 also decreased serum creatinine levels in a concentration dependent manner. Hematoxylin–eosin (H&E) staining was per-
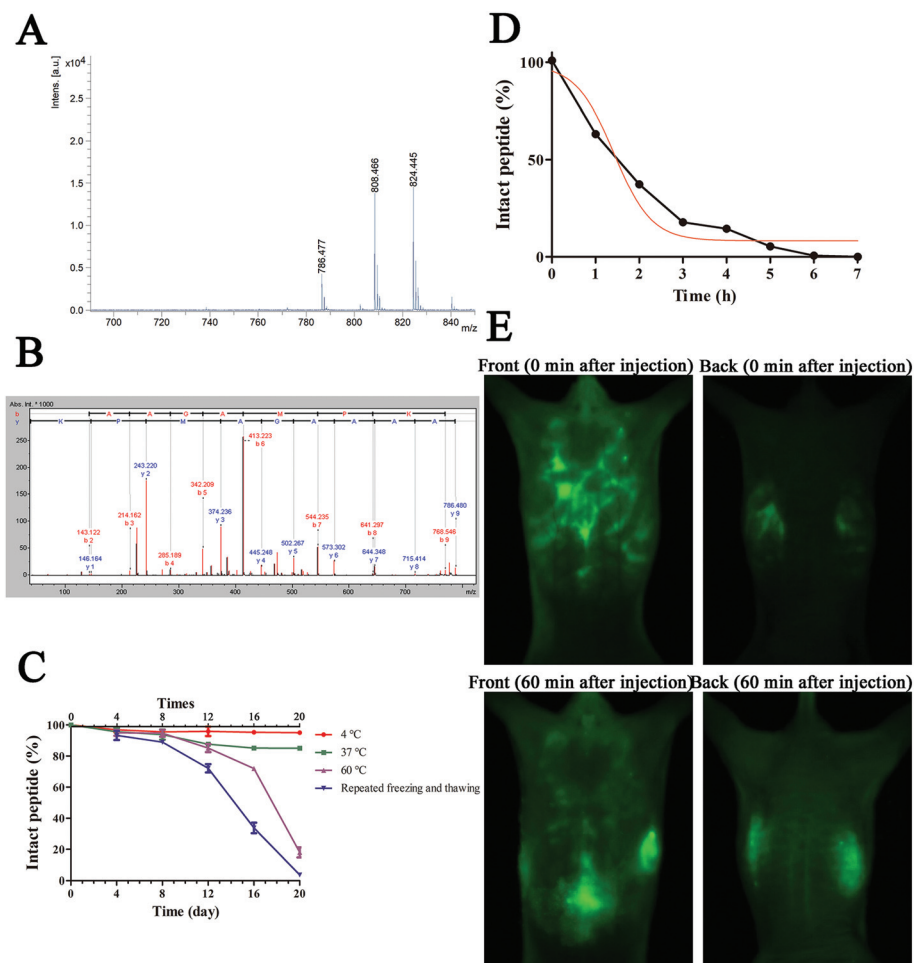
Fig. 1 RDP2 showed good stability under various conditions and was primarily distributed in the liver and kidneys. (A) Mass spectrometry of RDP2. (B) Primary structure of RDP2 (AAAAGAPMK-NH2). (C) Stability of RDP2 at 4 °C, 37 °C, and 60 °C, and after repeated freezing and thawing (n = 3). (D) RDP2 remained in plasma for 7 h, with a half-life of 1.4 h (n = 3). (E) Distribution of RDP2 in mice after injection.

formed to evaluate the effects of RDP2 in alleviating renal damage induced by HUA. As seen in Fig. 3, the control group showed clear renal tubule borders and orderly arranged epithelial cells. In contrast, the HUA mouse kidneys showed diminished brush borders, indistinct boundaries between adjacent proximal convoluted tubules, and tubular atrophy. However, both RDP2 and positive control treatments relieved the renal pathological changes observed in HUA mice to a certain extent.

Bioinformatics analysis of liver and kidneys in HUA mice

High-throughput sequencing was carried out on the livers and kidneys of HUA mice to understand the mechanism related to anti-hyperuricemia using RDP2. The liver detection results identified 1717 differentially expressed genes (DEGs) between the RDP2 and model groups, including 738 up-regulated and 979 down-regulated genes (Fig. 4A and B). The kidney detection results identified 2470 DEGs between the treatment and model groups, including 1389 up-regulated genes and 1081 down-regulated genes (Fig. 4C and D). Bioinformatics analysis was used to compare, analyze, and screen the relevant data.

Results showed that xanthine dehydrogenase (XDH, EC: 1.17.1.4), XOD (EC: 1.17.3.2), uricase (EC: 1.7.3.3), and SLC22A12-gene-encoded URAT1 were down-regulated, as was the *GBP5* gene (which affects the position regulation of NLRP3 inflammasome complex assembly).

Molecular docking

Based on the sequencing results, molecular docking was performed to analyze the mechanism related to uric acid reduction by simulating the docking of RDP2 with XOD and URAT1. As shown in Fig. S2A–D,† RDP2 was combined in the large cavity of XOD, and the binding affinity was −7.4 kcal mol⁻¹. As shown in Fig. S2E–H,† RDP2 was bound in a more extended conformation to the hydrophobic core surrounded by a spiral structure in URAT1, with an affinity of −8.2 kcal mol⁻¹.

RDP2 inhibited XOD activity and URAT1 expression in HUA mice

To verify the directly reaction of RDP2 and XOD, the XOD inhibition assay *in vitro* was performed. As shown in Fig. S3,†
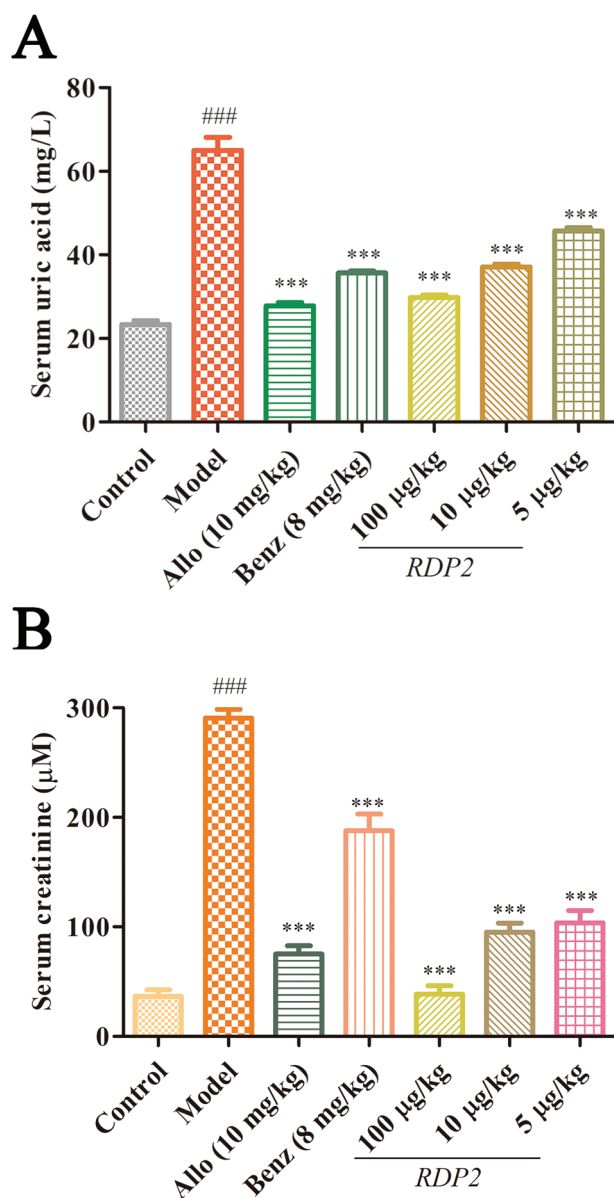
Fig. 2 RDP2 decreased serum uric acid and creatinine levels in hyper-uricemic mice. (A) RDP2 decreased serum uric acid in hyperuricemic mice concentration dependently ($n = 6$). (B) RDP2 significantly reduced serum creatinine level in mice ($n = 6$). ***$p < 0.001$ indicates significantly different from control (Student's t-test).

Fig. 3 RDP2 alleviated tissue damage in mice. Control group showed orderly arranged epithelial cells. Model group showed brush border disappearance and tubular atrophy. Treatment with RDP2 and positive control relieved renal injury to a certain extent.

RDP2 showed XOD inhibition activity *in vitro* in a concentration dependent manner. RDP2s (100 μg mL^{-1}) inhibiting activity against XOD were 1/6 that of Allo (10 mg mL^{-1}) ($n = 5$).

XOD activity in HUA mice was then tested. As shown in Fig. 5A and B, HUA caused an abnormal increase in XOD activity *in vivo* of mice, which was alleviated by the Allo treatment, and the RDP2 treatment effectively reduced serum and liver XOD activities in HUA mice ($P < 0.001$). The expression level of URAT1 in the kidneys was also measured. As shown in Fig. 5C, compared with the control group, the expression of URAT1 in the model group increased significantly, and with
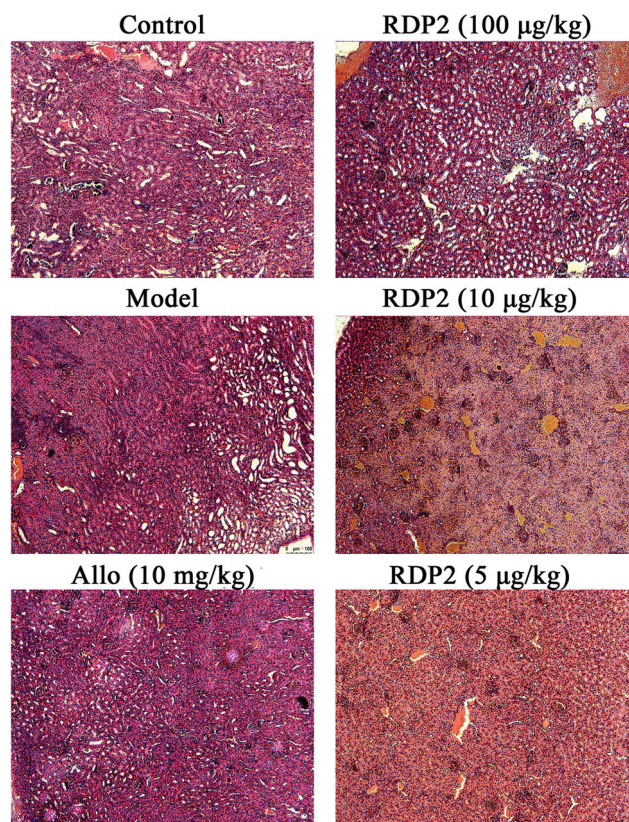
the intervention of Benz, the expression of URAT1 was similar to that in the control group. Moreover, the RDP2 treatment (5, 10, and 100 μg kg^{-1}) significantly decreased the expression of URAT1 in the kidneys.

RDP2 alleviated renal damage by decreasing kidney inflammation

The accumulation of uric acid in the kidneys can cause repeated inflammation, leading to kidney damage.[24] The content of IL-1β in the serum of HUA mice was first tested. As shown in Fig. 5D, the IL-1β content was three times higher in the model group than that in the normal group, suggesting that HUA led to the enhancement of inflammatory responses in mice. In the Allo and RDP2 (5, 10, and 100 μg kg^{-1}) groups, the serum IL-1β content in HUA mice was successfully reduced. The production of IL-1β mainly depends on NLRP3 inflammasomes (NLRP3, ASC, and caspase-1).[25] Therefore, NLRP3 inflammasome expression in the kidneys of HUA mice was detected by western blot analysis. As shown in Fig. 5E–H, RDP2 (100 μg kg^{-1}) significantly decreased NLRP3 inflammasome expression (NLRP3, ASC, and caspase-1).
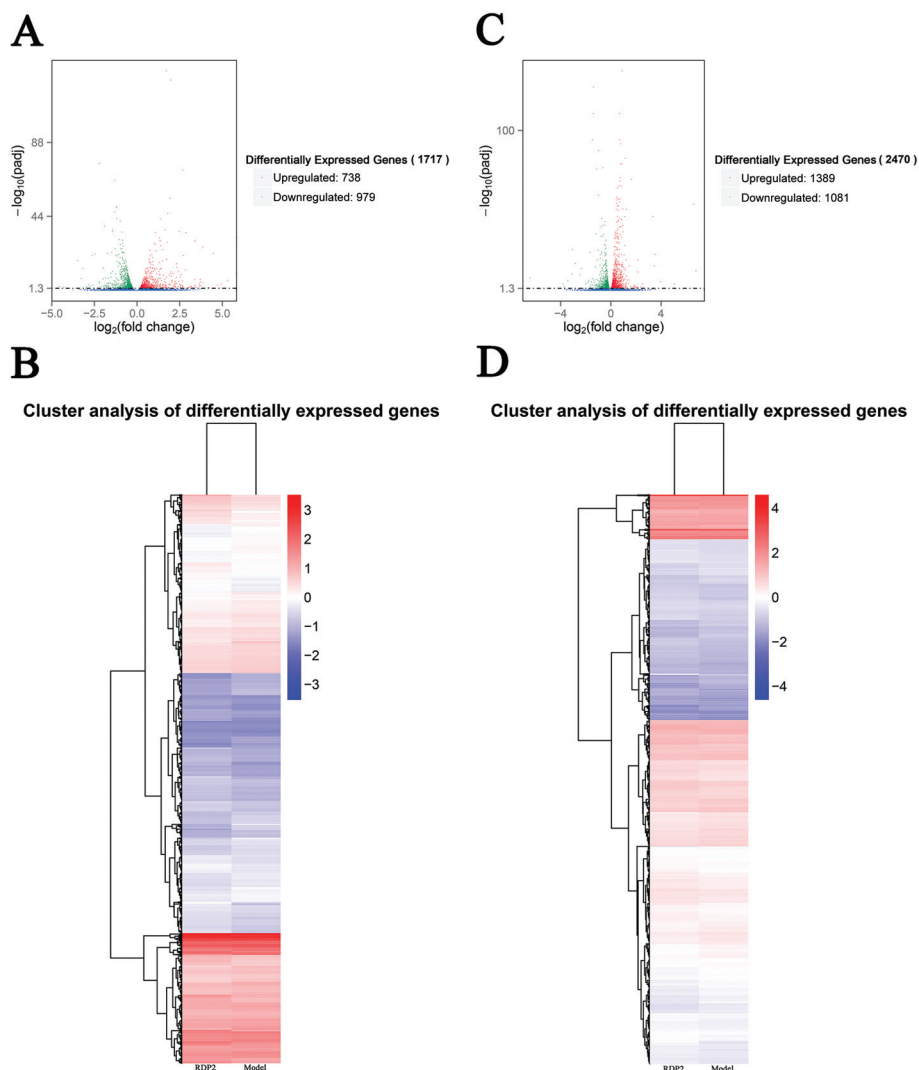
Fig. 4 Comparison of differentially expressed genes (DEGs) between RDP2-treated and model mice. Based on transcriptome analysis of livers and kidneys of mice (RDP2 group *vs.* model group), liver detection (A and B) identified 1717 DEGs between RDP2 and model groups, including 738 up-regulated and 979 down-regulated genes, and kidney detection (C and D) identified 2470 DEGs between the two groups, including 1389 up-regulated genes and 1081 down-regulated genes (six mice per group, repeated three times in total).

RDP2 showed anti-inflammatory and analgesic activities

The effect of RDP2 on pain induced by inflammation was detected, as shown in Fig. S4.† At 15–30 min, RDP2 exposure (5, 10, and 100 μg kg^{-1}) resulted in significant and concentration-dependent pain relief, with RDP2 at 100 μg kg^{-1} exhibiting stronger analgesic capability than diclofenac sodium (DS, 12 mg kg^{-1}).

In the mouse paw swelling model induced by MSU, swelling peaked on the first day after injection, as shown in Fig. 6A. Compared with the control group, edema caused by MSU was significantly alleviated in the DS group (12 mg kg^{-1}) ($P <$ 0.001). The results showed that RDP2 demonstrated a significant and concentration-dependent ability to reduce swelling, with RDP2 at 100 μg kg^{-1} exhibiting a similar ability to that of DS at 12 mg kg^{-1}.

The levels of inflammatory factors in the paw were also measured. As shown in Fig. 6B and C, MSU injection induced an increase in TNF-α and IL-1β in the foot tissues of mice ($P <$ 0.001, Saline *vs.* Model), which was significantly improved by DS treatment (12 mg kg^{-1}). Results also showed that, compared with the Saline group, TNF-α content in the RDP2 groups (10 and 100 μg kg^{-1}) decreased; furthermore, the IL-1β content in the RDP2 groups (5, 10, and 100 μg kg^{-1}) showed a concentration-dependent reduction.

H&E staining was then carried out to evaluate changes in foot tissues after RDP2 treatment. As shown in Fig. 6D, tissues in the control group were closely arranged and exhibited normal cell morphology; whereas loose connective tissues in the model group were thickened and showed inflammatory cell recruitment. These results suggest that inflammation can
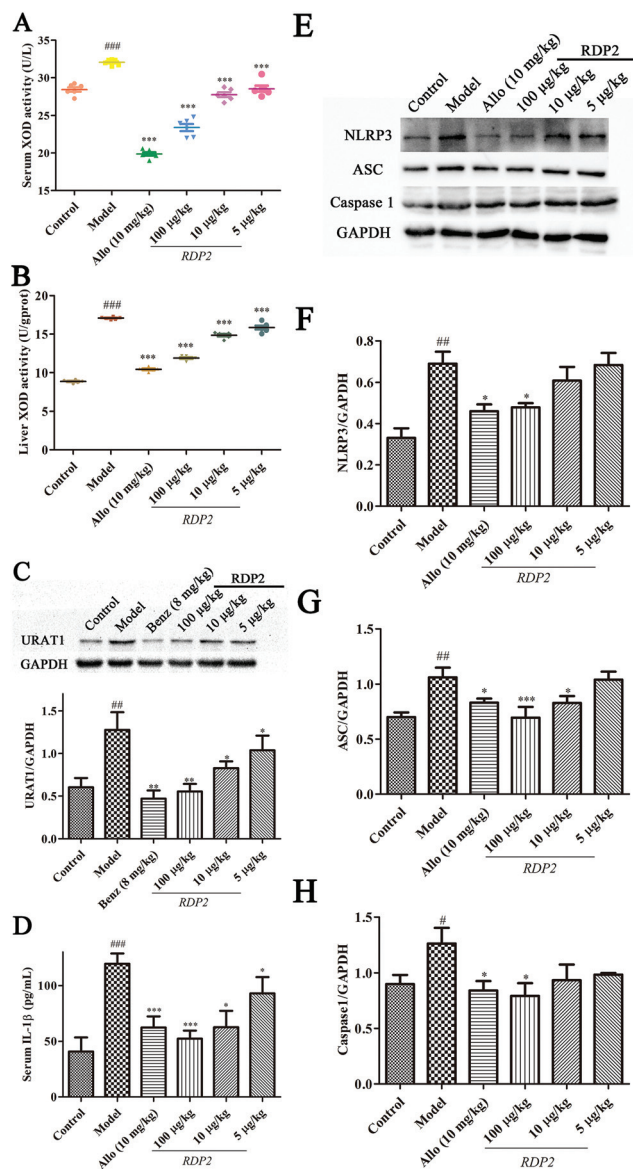
Fig. 5 RDP2 decreased XOD activity in mice and showed anti-inflammatory activity ($n = 3$). RDP2 decreased XOD activity in serum (A) and liver (B) in a concentration dependent manner ($n = 6$), and decreased expression of URAT1 in kidneys (C). RDP2 (5, 10, and 100 µg kg^{-1}) decreased serum level of IL-1β in mice in a concentration dependent manner (D). NLRP3 inflammasome expression in hyperuricemic mice was detected by western blot analysis, and results (E) were analyzed quantitatively. F–H show quantitative analysis, with RDP2 reducing NLRP3 inflammasome expression (NLRP3, ASC, and caspase-1). $^{\#}/^{*}p < 0.05$, $^{\#\#}/^{**}p < 0.01$, and $^{\#\#\#}/^{***}p < 0.001$ indicate significantly different from control (Student's t-test).

lead to pathological changes, which may be relieved by DS or RDP2 treatment.

Discussion

As a disease characterized by HUA and arthritis, gout can seriously affect quality of life in sufferers. Taking a preventive

approach to HUA in the early stages of gout is thus considered extremely important.[6] At present, however, gout and HUA medicine cannot solve clinical needs. Therefore, the development of novel drug candidates with a wide range of effects to fight and prevent gout is critical. In this study, we identified a plant-derived peptide, named RDP2, which not only reduced uric acid via dual targets and alleviated renal damage, but also reduced inflammation during acute gout attack.

HUA is the biochemical basis of gout and plays an important role in associated complications, such as hypertension, chronic kidney disease, and metabolic syndrome, and the accumulation of uric acid can also cause serious damage to organs such as the kidneys.[24,25] Under normal physiological conditions, purine is metabolized in the liver, where it produces uric acid with the action of various enzymes (such as XOD).[26] Uric acid is then primarily excreted via the kidney and renal transporters (reabsorption and secretory transporters) located in the proximal convoluted tubules.[27] This also makes XOD and URAT1 important targets in the treatment of HUA.

In this study, RDP2 was obtained from water extract of shelled *O. sativa* fruits by peptide histochemistry (Fig. 1A, B and S1†). The peptide exhibited no hemolytic activity or acute toxicity (Tables S1 and S2†). Furthermore, as shown in Fig. 1C, it could be maintained long-term at 4 °C and 37 °C and short-term at 60 °C. RDP2 also showed good stability in plasma (half-life of 1.4 h, Fig. 1D). In a previous study, an anti-hyperuricemia peptide (RDP1, AAAAGAKAR) was identified, which was completely degraded in the plasma for 20 min, with a half-life of 4.6 min, with RDP2 showing a stronger plasma stability (half-life: 1.4 h), which may be due to the existence of post-translational modification (-NH2), and the stability test results in other cases also confirm the better stability of RDP2 than that of RDP1.[16] These characteristics suggest good advantages for the transportation and preservation of RDP2, and also indicate the benefits for long-term maintenance *in vivo*.

In HUA mice, RDP2 exposure induced a significant and concentration-dependent reduction in serum uric acid and creatinine levels (Fig. 2). Moreover, RDP2 (100 µg kg^{-1}) showed stronger activity of reducing uric acid than that of Benz, and had similar activity to Allo ($P < 0.0001$, RDP2 vs. Benz). The results showed that RDP2 (100 µg kg^{-1}) also had stronger ability of reducing creatinine than that of Allo and Benz ($P < 0.01$, RDP2 vs. Allo; $p < 0.0001$, RDP2 vs. Benz). RDP2 also showed a stronger anti-hyperuricemic activity than that of RDP1, both in the reduction of uric acid and creatinine levels, and the maximun effective concentration of RDP2 (100 µg kg^{-1}) is much lower than that of RDP1 (1 mg kg^{-1}), which proved the superiority of RDP2 in structure and activity (the results of the model group were taken as 100%, and the reduction degree of uric acid and creatinine in the peptide groups were observed). The H&E staining results also showed that RDP2 alleviated renal injury induced by HUA (Fig. 3). In the current study, transcriptome sequencing showed that genes related to XOD, URAT1, and positive regulation of NLRP3 inflammasome complex assembly were down-regulated in HUA mice treated with RDP2 (Fig. 4). Thus, the anti-HUA
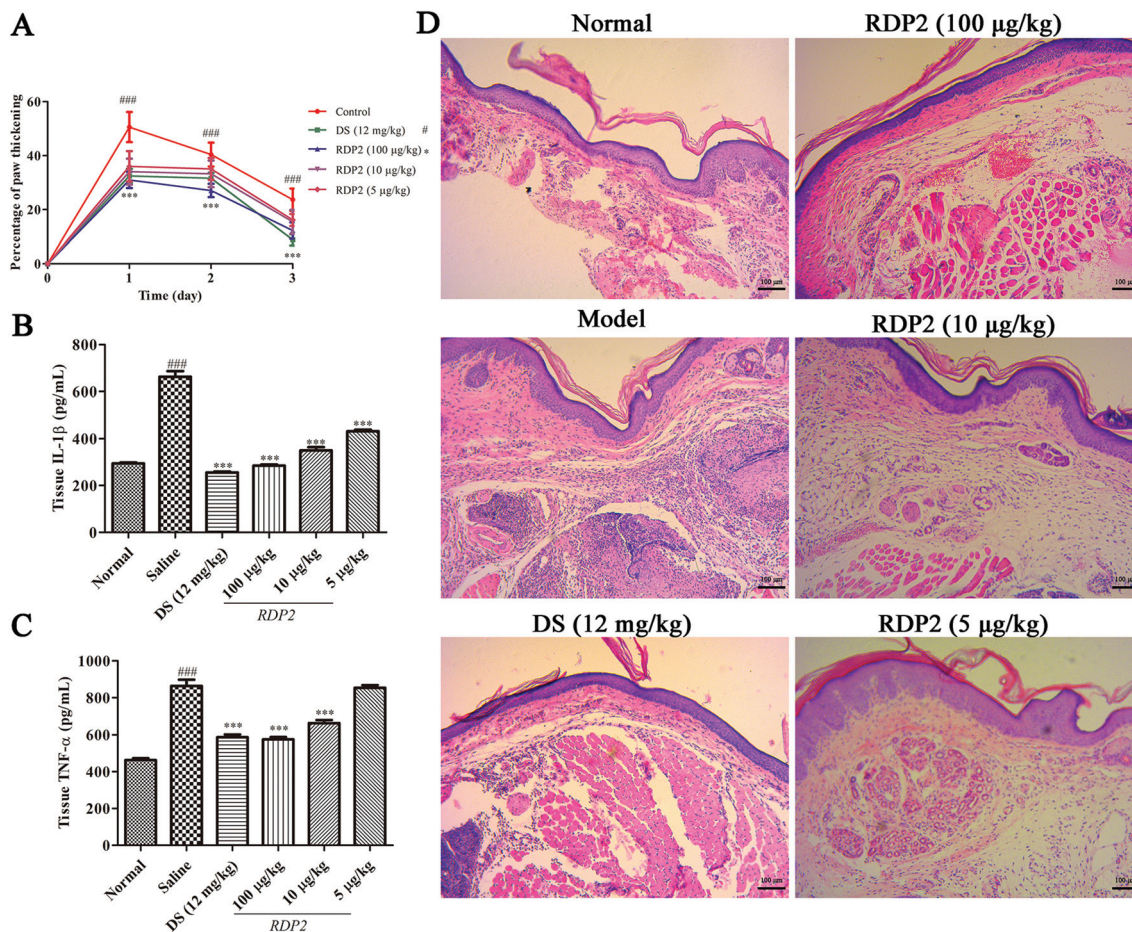
Fig. 6 RDP2 reduced foot swelling in mice injected with MSU and decreased inflammation. (A) RDP2 reduced paw swelling induced by MSU in a concentration dependent manner (n = 6). (B) RDP2 (5, 10, and 100 µg kg^{-1}) decreased tissue level of IL-1β in mouse paws in a concentration dependent manner (n = 6). (C) RDP2 (10 and 100 µg kg^{-1}) reduced serum level of TNF-α in mice (n = 6). (D) RDP2 alleviated tissue injury caused by MSU injection. [###]/[***]p < 0.001 indicates significantly different from control (Student's t-test).

and nephropathic ability of RDP2 may be achieved by inhibiting XOD, URAT1, and NLRP3 inflammasome complex assembly. As shown in Fig. S2,† the molecular docking results also showed good affinity for RDP2-XOD (−7.4 kcal mol^{-1}) and -URAT1 (−8.2 kcal mol^{-1}), and in the docking between RDP1 and XOD, the affinity was −10.2 kcal mol^{-1}. In XOD inhibition assay *in vitro* (Fig. S3†), at the maximum effective concentration, the inhibition rate of RDP2 (100 µg mL^{-1}) was half of that of RDP1 (1 mg mL^{-1}). The results indicated that RDP1 has better XOD inhibition activity than that of RDP2 *in vitro*, which was consistent with the results of molecular docking. *In vivo* experiments then showed that RDP2 effectively inhibited XOD activity in HUA mice and significantly down-regulated URAT1 expression in their kidneys, indicating that RDP2 may reduce uric acid by inhibiting its generation and reabsorption (Fig. 5A–C).

Under HUA conditions, excess uric acid stimulates tissues and causes inflammation, which plays a key role in HUA nephropathy.[28] Excessive accumulation of uric acid in the kidneys can activate the NLR family pyrin domain inflamma-

tory complex (*i.e.*, NLRP3 inflammasomes, composed of NLRP3, ASC, and pro-caspase-1). NLRP3 complex assembly induces the secretion of mature IL-1β, which leads to an increase in renal inflammation.[24,25] In the present study, we found that RDP2 treatment reduced the level of serum IL-1β in HUA mice (Fig. 5D). In addition, NLRP3 inflammasome expression (NLRP3, ASC, and caspase-1) was down-regulated in the kidneys of HUA mice treated with RDP2 (100 µg kg^{-1}) (Fig. 5E–H). These results indicate that RDP2 can reduce uric acid through multiple targets. RDP2 inhibited HUA and its related nephropathy by inhibiting XOD activity, decreasing URAT1 content, and alleviated renal damage by inhibiting NLRP3 inflammasome expression.

During the construction of the HUA model in mice, POX inhibits uricase and adenine increases purine intake and simulates HUA nephropathy.[16] Therefore, the anti-hyperuricemic effects of RDP2 may be due to its antagonism against the effects of POX. Interestingly, we found that RDP2 not only inhibited XOD activity and reduced the expression of URAT1, but also, based on high-throughput sequencing, down-regu-

lated the expression of uricase. Accordingly, we concluded that RDP2 showed anti-HUA activity by influencing the production and excretion of uric acid rather than by the loss of inhibition of urate oxidase.

Clinically, Allo and Benz are both used as first-line drugs for anti-HUA and are well-known for their rapid reduction of serum uric acid.[7] In this research, RDP2 (100 µg kg^{-1}) decreased serum uric acid and creatinine at a much lower treatment concentration than that of Allo or Benz (10 mg kg^{-1} and 8 mg kg^{-1}, respectively). It is worth noting that, among the approved anti-HUA drugs (including Allo and Benz) and other published anti-HUA peptides, none can inhibit both XOD and URAT1.[4,11,12,16,18,26] In addition, RDP2 was extracted from edible rice, and thus the risk of adverse reactions in humans should be low. These results all point to RDP2 as having excellent potential to be a new medicine candidate.

Long-term HUA can increase the accumulation and crystallization of urate in circulation, and eventually induce gout.[29] The symptoms of gout include an immune response to MSU stimulation, which is caused by the secretion of inflammatory cytokines such as IL-1β and TNF-α.[30] In this study, as shown in Fig. 6, RDP2 alleviated pain induced by formalin and inflammatory swelling caused by MSU, with peptide treatment (100 µg kg^{-1}) showing stronger activity than that of DS (12 mg kg^{-1}). Correspondingly, RDP2 also induced a concentration-dependent reduction in the content of IL-1β and TNF-α. Moreover, H&E staining showed that RDP2 treatment alleviated the recruitment of inflammatory cells and pathological changes in loose connective tissues. Therefore, as a novel anti-gout peptide, RDP2 could play a role not only in anti-HUA and renal protection, but also in anti-inflammation and analgesia.

Materials and methods

Sample purification and synthesis

Sample preparation. The shelled fruits of *O. sativa* were obtained from Yunnan, China, and were treated *via* the following steps:[16] the rice was soaked in 4 °C deionized water for 12 h, with the supernatant then obtained using filter paper. The supernatant was centrifuged for 20 min at 4 °C and 12 000*g*. The obtained liquid was then freeze-dried and stored at −80 °C.

Purification procedures. The separation and purification of the peptide was carried out according to our previous study.[31] The samples were separated using a Sephadex G-50 gel filtration column (1.5 × 31 cm, superfine, GE Healthcare, Sweden). The column was pre-balanced with 25 M Tris-HCl buffer containing 0.1 M NaCl (pH 7.8) and then the separation procedure was performed at a rate of 0.3 mL min^{-1} in the same buffer. The eluted components were collected in tubes every 10 min using an automatic fractionation collector (BSA-30A, HuXi Company, Shanghai, China) and their absorbance at 280 nm was detected (Fig. S1A,† as in our previous research[16]). The samples indicated by an arrow in Fig. S1A† were combined, and then further separated and purified by

RP-HPLC with an injection volume of 1 mL. A C18 HPLC column (Hypersil BDS C18, 4.0 × 300 mm, Elite, China) was used during operation, and was pre-balanced with ultra-pure water containing 0.1% (V/V) trifluoroacetic acid (TFA) and a buffer of acetonitrile (ACN) containing 0.1% (V/V) TFA, which was eluted *via* a linear gradient (0%–40% ACN, 40 min, Fig. S1B,† as reported in our previous study[16]). The purification procedure was conducted at a flow rate of 1 ml min^{-1} with a detection wavelength of 220 nm. Finally, the sample showing a peak in Fig. S1C† (as indicated by an arrow) was collected and purified *via* a second cycle of HPLC under the same conditions as the first step.

Determination of the peptide primary structure. The molecular mass of the purified sample was detected by mass spectrometry. In total, 1 µl of sample was mixed with an equal volume of α-cyano-4-hydroxycinnamic acid (5 mg ml^{-1}, dissolved in 50% ACN, 0.1% TFA) and spotted on a steel plate for crystallization. The plate underwent MS and MS/MS analysis using a mass spectrometer (Autoflex speed TOF/TOF, Bruker Daltonik GmbH, Leipzig, Germany) under a positive charge mode.

Synthesis of peptide. The RDP2 peptide (AAAAGAMPK-NH2) with a purity of >95% was commercially synthesized by Wuhan Bioyeargene Biotechnology Co., Ltd (Wuhan, China).

Animal care

Adult Kunming mice (male and female) and nude mice (male) (25 ± 5 g) were both obtained from Hunan Slack Jingda Experimental Animal Co., Ltd (Hunan, China) (male Kunming mice were used to establish hyperuricemia and the gout animal model; male and female Kunming mice were used for acute toxicity assays; and male nude mice were used for the distribution of RDP2 assays). The mice were maintained in cages (330 × 205 × 180 mm, 3 mice per cage) at room temperature (22 ± 2 °C) and provided with food and water *ad libitum*. All animal handling was conducted in accordance with the Provision and General Recommendation of Chinese Experimental Animals Administration Legislation. All animal care and handling procedures were performed in strict adherence to the requirements of the Ethics Committee of Kunming Medical University, Yunnan, China (KMMU20180012).

Characteristics of RDP2

Hemolytic activity and acute toxicity assays. Hemolytic activity and acute toxicity tests followed previous research, with some modifications.[31] Briefly, to obtain 100% red blood cells, human red blood cells obtained from the Kunming Institute of Zoology (Yunnan, China) were washed three times with saline. Different doses of RDP2 (5, 10, and 100 µg mL^{-1}) were mixed with the red blood cells, followed by incubation at 37 °C for 30 min. The mixtures were then centrifuged at 4000*g* for 4 min at room temperature (22 ± 2 °C), with the subsequent supernatant collected and measured for absorbance at 540 nm. Maximum hemolysis was determined using 1% Triton X-100. Either RDP2 (5, 10, or 100 µg mL^{-1}) or saline was

injected into mice, with mortality, toxicity, and behavioral changes of mice observed and recorded over 24 h.

Stability of RDP2. The stability of RDP2 was determined according to a previous report.[16] In total, 100 μL of mouse plasma and 100 μl of RDP2 (10 μg mL^{-1}) were mixed and incubated at 37 °C, then tested every 2 h until the peptide was completely degraded. Then, 219 μL of urea (8 M) and 60 μL of trichloroacetic acid (1 g mL^{-1}) were added to the mixture to terminate the reaction, followed by centrifugation at 12 000g for 30 min at 4 °C. The resulting supernatant was collected to test the amount of peptide by HPLC.

RDP2 (10 μg mL^{-1}) was frozen at −20 °C overnight and thawed at 37 °C (repeatedly), after which the residual peptide was detected. The stability of RDP2 at 4 °C, 37 °C, and 60 °C was also determined. In brief, RDP2 (10 μg mL^{-1}) was incubated at 4 °C, 37 °C, and 60 °C for 20 days, and the samples were taken every 2 days and then centrifuged at 12 000g for 20 min at 4 °C to obtain the supernatant, which was then tested by HPLC.

Distribution of RDP2 *in vivo* after injection. Samples (FITC-AAAAGAMPK-NH2) were provided commercially by Wuhan Bioyeargene Biotechnology Co., Ltd (Wuhan, China). First, the nude mice were anesthetized with pentobarbital sodium (3.5%, 100 μL per 10 g) and then fixed. In total, 100 μL of FITC-RDP2 (10 μg μL^{-1}) was injected into the nude mice *via* the abdomen. After this, front and back images were taken and observed at 0 min and 60 min after injection, respectively, using a FluorVivo™ 300 (Huanya Technology Co., Ltd, Beijing, China).

Anti-hyperuricemic activity of RDP2

Establishment of HUA mice. Animal assays were performed according to previous research with some modifications.[32] Briefly, mice were randomly divided into seven groups (*i.e.*, control, model, two positive (allopurinol (Allo) and benzbromarone (Benz)), and three RDP2 groups (5, 10, and 100 μg kg^{-1}), n = 6). The control group was administered 1 mL of saline per day. Other groups were administered 300 mg kg^{-1} potassium oxonate (POX, Dalian Meilun Biological Technology Co., Ltd, Dalian, Liaoning, China) and 200 mg kg^{-1} adenine (Dalian Meilun Biological Technology Co., Ltd, Dalian, Liaoning, China) per day (intragastric administration). RDP2 or Allo/Benz was administered to mice by intraperitoneal injection 1 h after POX and adenine treatment. The control and model groups were treated with saline, and the positive groups were treated with Allo (10 mg kg^{-1}, Dalian Meilun Biological Technology Co., Ltd, Dalian, Liaoning, China) or Benz (8 mg kg^{-1}, Dalian Meilun Biological Technology Co., Ltd, Dalian, Liaoning, China). The RDP2 groups were treated with different concentrations of RDP2 (5, 10, or 100 μg kg^{-1}). POX and adenine were dissolved in saline, and mice were treated daily with POX and adenine or saline (control) for 7 d by intragastric administration. Blood and tissue samples were obtained on day 7 after the last administration of RDP2, Allo, or saline. Mice were anesthetized with 0.3% pelltobarbitalum natricum and blood was taken from the inner canthus vein, after which

liver and kidney tissues were quickly obtained on ice. The blood samples were centrifuged at 6000g at room temperature (22 ± 2 °C) for 5 min to obtain the serum. The livers of mice were stored at −80 °C. The kidneys of mice were divided into two parts, one part was stored at −80 °C and one part was fixed in 4% formaldehyde.

Detection of uric acid and creatinine levels in HUA mice serum. The serum levels of uric acid and creatinine were measured using specific uric acid and creatinine kits in accordance with the instructions provided by the Nanjing Jiancheng Bioengineering Institute (Nanjing, Jiangsu, China).

Hematoxylin–eosin (H&E) staining of kidneys. H&E staining was performed according to previous research.[33] Kidney tissues obtained from mice were fixed in 4% formalin for 24 h, and then dehydrated with gradient ethanol (75% 12 h, 85% 12 h, and 95% and 100% 2 h respectively). The tissues were then embedded in paraffin and sliced to a thickness of 5 μm for H&E staining. The sections were visualized under a light microscope (Zeiss, Germany) at 100× magnification.

Analysis of quantification and differential expression of transcripts. mRNA was enriched with magnetic beads.[34–36] Fragment buffer was added to break the mRNA into short fragments, which were then used as templates to enrich the cDNA library by polymerase chain reaction (PCR). The different libraries were sequenced by HiSeq/MiSeq. After obtaining sequence reads, biological information analysis was carried out based on reference sequences or genomes of related species. HTSeq software was used to analyze the gene expression level of each sample, and the number of differentially expressed genes (DEGs) and expression level of single genes were determined. For the samples with biological duplication, negative binomial distribution was used as the model and DESeq was used for the analysis. The RPKM (reads per kilo bases per million reads) values of gene expression levels were estimated. Hierarchical clustering analysis was carried out, with different colored regions representing different clustering information.

Molecular docking. Molecular docking of the RDP2-XOD and RDP2-URAT1 complexes was conducted to clarify potential binding.[37] The structure of XOD was downloaded online (ID number: 2ckj) (http://www.rcsb.org/pdb). For the crystal structure, crystal water and small molecules were deleted and Fe–S clusters and coenzymes were preserved, with the resulting structure saved in PDB format. The architecture of URAT1 was modeled from scratch using the Robetta server (http://www.robetta.org/) and the highest score was selected as the docking receptor after qualification using the pull chart. The receptor protein was loaded into autodocktool to automatically allocate atomic type and charge, and then saved in pdbqt format. The 3D structure of the RDP2 peptide was constructed using the PEPFORD 3 online server (http://bioserv.rpbs.univ-paris-diderot.fr/services/PEP-FOLD3/), with the best conformation then selected as the structure. Because of post-translation modification (-NH2) in RDP2, the amide group was added to

the structure of RDP2 using DS3.5 software, which was optimized and then saved in PDB format. Vina v1.1.2 was used for docking and conformation, with the one showing the best affinity selected as the docking conformation, which was then analyzed in PyMOL.

XOD activity *in vitro* and *in vivo*. XOD inhibition assay *in vitro* was carried out according to the literature with some modification (n = 5).[11] 50 mM Tris-HCl buffer (pH 8) was prepared as the solvent and negative control. Then 2 mM xanthine (Dalian Meilun Biological Technology Co., Ltd, Dalian, Liaoning, China) solution and 0.52 mM XOD (Dalian Meilun Biological Technology Co., Ltd, Dalian, Liaoning, China) solution was prepared. The xanthine solution (128 μL), XOD solution (16 μL), sample solution (32 μL, RDP2) and Tris-HCl buffer (928 μL) were mixed and incubated at 37 °C for 15 min, then the reaction was terminated with 48 μL 1 M HCl and the absorbance at 292 nm was detected. Allo (10 mg mL^{-1}) was used as the positive control. The inhibitory activity was calculated as follows:

$$\text{XOD inhibition rate}(\%) = 100\% \times \frac{\text{Negative control} - \text{Sample}}{\text{Negative control}}$$

XOD activities in the serum and liver were measured using XOD kits (Nanjing Jiancheng Bioengineering Institute, Nanjing, Jiangsu, China). All operations were carried out according to the instructions provided by the test kits.

Serum IL-1β content in HUA mice. Serum IL-1β levels of HUA mice were tested by using mouse IL-1β ELISA kits (Shenzhen NeoBioscience Biotechnology Co., Ltd, Shenzhen, China). All operations were carried out according to the instructions provided by the test kits.

Western blotting. Western blotting was used to detect protein expression in the kidneys of HUA mice.[38] Tissues were treated with 20 mg per 150 μl RIPA and PMSF (Dalian Meilun Biotechnology Co., Ltd, Dalian, Liaoning, China) at 100 : 1. The mixture was then centrifuged at 4 °C for 5 min at 12 000g. The supernatant was collected and detected using a BCA protein analysis kit (Dalian Meilun Biotechnology Co., Ltd, Dalian, Liaoning, China). The URAT1 and NLRP3 inflammasome contents were determined using sulfate polyacrylamide gel electrophoresis (SDS-PAGE) and western blotting. Each group of proteins was separated by 10% SDS-PAGE and transferred to polyvinylidene fluoride membranes, which were then sealed with 5% skimmed milk for 2 h at room temperature (22 ± 2 °C), then with primary antibody (GAPDH, URAT1, Proteintech, Shanghai Sixin Biotechnology Co., Ltd, Shanghai, China) at 4 °C overnight and then with secondary antibody (anti-rabbit, Proteintech, Shanghai Sixin Biotechnology Co., Ltd, Shanghai, China) for 1 h. ImageJ software was used to detect, analyze, and quantify specific frequency bands.

Anti-gout activity of RDP2

Anti-inflammatory and analgesic activities of RDP2. Different concentrations of RDP2 (5, 10, and 100 μg kg^{-1}) were intraperitoneally injected into mice.[39] The negative group received saline and the positive group received diclofenac sodium (DS, 12 mg kg^{-1}, NSAIDs). At 30 min after injection, 20 μL of 0.9% formalin was injected into the center of the right paw of mice, which were then placed in cages (20 × 40 × 15 cm) for observation. The time spent licking or patting paws from 0–5 min and 15–30 min after formalin injection was recorded.

The MSU crystal was prepared according to earlier literature.[40] In brief, 1 g of uric acid and 0.5 g of NaOH were dissolved into 100 mL of deionized water and incubated at 80 °C for 20 min, followed by cooling to room temperature and then to 4 °C overnight. The solution was adjusted to a pH of 7.2 and centrifuged at 1500g for 3 min at 4 °C to obtain the MSU crystal precipitate. The crystal was dried at 60 °C and then prepared to a concentration of 20 mg mL^{-1}.

The mice were divided into five groups (n = 6 per group). The model group was given saline (50 μL); positive control group was given DS (12 mg kg^{-1}); and three RDP2 groups were given different doses of RDP2 (5, 10, and 100 μg kg^{-1}). The mice were injected intraperitoneally once a day for 3 d. At 30 min after the last injection, 50 μL of MSU suspension was injected into the right paw of each mouse. At 1, 2, and 3 d after MSU injection, the thicknesses of the paws were measured using a digital thickness meter (Hong Kong Dinghao Measuring Tool Co., Ltd, Hong Kong, China). The percentage of edema was calculated as follows:

$$\text{Swelling rate}(\%) = 100\% \times \frac{B - A}{A}$$

where A is the paw thickness before injection and B is the paw thickness after injection.

Paw inflammatory cytokine assays and H&E staining. The levels of IL-1β and TNF-α in foot tissue samples from mice were determined using mouse IL-1β and TNF-α ELISA kits in accordance with the protocols provided by Shenzhen NeoBioscience Biotechnology Co., Ltd (Shenzhen, China).

H&E staining of the paws was performed following the same procedures as used for the kidneys.

Conclusions

In summary, we obtained an active peptide, RDP2, from water extract of shelled *O. sativa* fruits, which had a novel structure, no toxic side effects, and excellent stability. RDP2 is a multitarget anti-hyperuricemic peptide, which was able to inhibit XOD and URAT1 expression at a relatively low concentration (100 μg kg^{-1}, 10 μg kg^{-1} and 5 μg kg^{-1}). It also reduced renal inflammatory damage in HUA mice, and showed excellent anti-inflammatory and analgesic abilities. Thus, this plant-derived anti-hyperuricemia peptide which may also alleviate the acute attack of gout exhibited a wide range of activities and remarkable effects, which should provide options for the development of anti-gout drugs.

Author contributions

X. W. Y. and Y. W. designed the study; N. X. L. and B. L. M. performed most of the research, including data collection, purification procedures, peptide structure determination, data analysis, and manuscript composition; L. Z., S. G. Y., and Y. H. participated in the purification procedures; and S. S. L., X. P. Z. and Y. F. participated in the anti-hyperuricemic activity determination of the peptide. M. F. Y., L. J. S. and C. X. participated in the mechanism research. All authors contributed substantially to this research and reviewed this manuscript.

Conflicts of interest

There are no conflicts to declare.

Acknowledgements

References

1 C. M. Burns and R. L. Wortmann, Gout therapeutics: new drugs for an old disease, *Lancet*, 2011, **377**, 165–177.
2 T. Pascart and F. Lioté, Gout: state of the art after a decade of developments, *Rheumatology*, 2019, **58**(1), 27–44.
3 Y. Zhang, H. Zhang, D. Chang, F. Guo, H. Pan and Y. Yang, Metabolomics approach by (1)H NMR spectroscopy of serum reveals progression axes for asymptomatic hyperuricemia and gout, *Arthritis Res. Ther.*, 2018, **20**, 111.
4 W. He, G. Su, D. Sun-Waterhouse, G. I. N. Waterhouse, M. Zhao and Y. Liu, In vivo anti-hyperuricemic and xanthine oxidase inhibitory properties of tuna protein hydrolysates and its isolated fractions, *Food Chem.*, 2019, **272**, 453–461.
5 X. Li, Z. Yan, M. Carlstrom, J. Tian, X. Zhang, W. Zhang, S. Wu and F. Ye, Mangiferin Ameliorates Hyperuricemic Nephropathy Which Is Associated With Downregulation of AQP2 and Increased Urinary Uric Acid Excretion, *Front. Pharmacol.*, 2020, **11**, 49.
6 P. P. Khanna, Gout: a patrician malady no more, *Lancet Diabetes Endocrinol.*, 2018, **6**, 263–264.
7 Q. Zhou, J. Su, T. Zhou, J. Tian, X. Chen and J. Zhu, A study comparing the safety and efficacy of febuxostat, allopurinol, and benzbromarone in Chinese gout patients: a retrospective cohort study, *Int. J. Clin. Pharmacol. Ther.*, 2017, **55**, 163–168.
8 K. L. Martens, P. R. Khalighi, S. Li, A. A. White, E. Silgard, D. Frieze, E. Estey, D. A. Garcia, S. Hingorani and A. Li, Comparative effectiveness of rasburicase versus allopurinol for cancer patients with renal dysfunction and hyperuricemia, *Leuk. Res.*, 2020, **89**, 106298.
9 A. Bensman, Non-steroidal Anti-inflammatory Drugs (NSAIDs) Systemic Use: The Risk of Renal Failure, *Front. Pediatr.*, 2019, **7**, 517.
10 R. Bao, M. Liu, D. Wang, S. Wen, H. Yu, Y. Zhong, Z. Li, Y. Zhang and T. Wang, Effect of Eurycoma longifolia Stem Extract on Uric Acid Excretion in Hyperuricemia Mice, *Front. Pharmacol.*, 2019, **10**, 1464.
11 I. Murota, S. Taguchi, N. Sato, E. Y. Park, Y. Nakamura and K. Sato, Identification of antihyperuricemic peptides in the proteolytic digest of shark cartilage water extract using in vivo activity-guided fractionation, *J. Agric. Food Chem.*, 2014, **62**, 2392–2397.
12 Q. Li, X. Kang, C. Shi, Y. Li, K. Majumder, Z. Ning and J. Ren, Moderation of hyperuricemia in rats via consuming walnut protein hydrolysate diet and identification of new antihyperuricemic peptides, *Food Funct.*, 2018, **9**, 107–116.
13 S. K. Paul, D. Maggs, K. Klein and J. H. Best, Dynamic risk factors associated with non-severe hypoglycemia in patients treated with insulin glargine or exenatide once weekly, *J. Diabetes*, 2015, **7**, 60–67.
14 S. Malhan, S. Guler, I. Yetkin, S. Baeten and B. Verheggen, Cost-Effectiveness of Exenatide Twice Daily (Bid) Added To Basal Insulin Compared To A Bolus Insulin Add-On In Turkey, *Value Health*, 2014, **17**, A349.
15 S. Higuchi, N. Murayama, K. Saguchi, H. Ohi, Y. Fujita, N. J. da Silva Jr., R. J. de Siqueira, S. Lahlou and S. D. Aird, A novel peptide from the ACEI/BPP-CNP precursor in the venom of Crotalus durissus collilineatus, *Comp. Biochem. Physiol., Part C: Toxicol. Pharmacol.*, 2006, **144**, 107–121.
16 N. Liu, Y. Wang, M. Yang, W. Bian, L. Zeng, S. Yin, Z. Xiong, Y. Hu, S. Wang, B. Meng, J. Sun and X. Yang, New Rice-Derived Short Peptide Potently Alleviated Hyperuricemia Induced by Potassium Oxonate in Rats, *J. Agric. Food Chem.*, 2019, **67**, 220–228.
17 D. Kubomura, M. Yamada and A. Masui, Tuna extract reduces serum uric acid in gout-free subjects with insignificantly high serum uric acid: A randomized controlled trial, *Biomed. Rep.*, 2016, **5**, 254–258.
18 Y. Li, X. Kang, Q. Li, C. Shi, Y. Lian, E. Yuan, M. Zhou and J. Ren, Anti-hyperuricemic peptides derived from bonito hydrolysates based on in vivo hyperuricemic model and in vitro xanthine oxidase inhibitory activity, *Peptides*, 2018, **107**, 45–53.
19 Y. Ma, H. Cao, Z. Li, J. Fang, X. Wei, P. Cheng, R. Jiao, X. Liu, Y. Li, Y. Xing, J. Tang, L. Jin and T. Li, A Novel Multi-Epitope Vaccine Based on Urate Transporter 1 Alleviates Streptozotocin-Induced Diabetes by Producing Anti-URAT1 Antibody and an Immunomodulatory Effect in C57BL/6J Mice, *Int. J. Mol. Sci.*, 2017, **18**, 2137.
20 K. A. Zoghebi, E. Bousoik, K. Parang and K. A. Elsaid, Design and Biological Evaluation of Colchicine-CD44-

Targeted Peptide Conjugate in an In Vitro Model of Crystal Induced Inflammation, *Molecules*, 2019, **25**, 46.

21 I. Galvao, J. P. Vago, L. C. Barroso, L. P. Tavares, C. M. Queiroz-Junior, V. V. Costa, F. S. Carneiro, T. P. Ferreira, P. M. Silva, F. A. Amaral, L. P. Sousa and M. M. Teixeira, Annexin A1 promotes timely resolution of inflammation in murine gout, *Eur. J. Immunol.*, 2017, **47**, 585–596.

22 V. Vanheule, R. Janssens, D. Boff, N. Kitic, N. Berghmans, I. Ronsse, A. J. Kungl, F. A. Amaral, M. M. Teixeira, J. Van Damme, P. Proost and A. Mortier, The Positively Charged COOH-terminal Glycosaminoglycan-binding CXCL9(74-103) Peptide Inhibits CXCL8-induced Neutrophil Extravasation and Monosodium Urate Crystal-induced Gout in Mice, *J. Biol. Chem.*, 2015, **290**, 21292–21304.

23 W. M. Mackin, S. M. Rakich and C. L. Marshall, Inhibition of rat neutrophil functional responses by azapropazone, an anti-gout drug, *Biochem. Pharmacol.*, 1986, **35**, 917–922.

24 J. Han, X. Wang, S. Tang, C. Lu, H. Wan, J. Zhou, Y. Li, T. Ming, Z. J. Wang and X. Su, Protective effects of tuna meat oligopeptides (TMOP) supplementation on hyperuricemia and associated renal inflammation mediated by gut microbiota, *FASEB J.*, 2020, **34**, 5061–5076.

25 D. Cui, S. Liu, M. Tang, Y. Lu, M. Zhao, R. Mao, C. Wang, Y. Yuan, L. Li, Y. Chen, J. Cheng, Y. Lu and J. Liu, Phloretin ameliorates hyperuricemia-induced chronic renal dysfunction through inhibiting NLRP3 inflammasome and uric acid reabsorption, *Phytomedicine*, 2020, **66**, 153111.

26 A. B. Nongonierma and R. J. Fitzgerald, Tryptophan-containing milk protein-derived dipeptides inhibit xanthine oxidase, *Peptides*, 2012, **37**, 263–272.

27 C. Li, L. Han, A. M. Levin, H. Song, S. Yan, Y. Wang, Y. Wang, D. Meng, S. Lv, Y. Ji, X. Xu, X. Liu, Y. Wang, L. Zhou, Z. Miao and Q. S. Mi, Multiple single nucleotide polymorphisms in the human urate transporter 1 (hURAT1) gene are associated with hyperuricaemia in Han Chinese, *J. Med. Genet.*, 2010, **47**, 204–210.

28 S. Lee, W. Kim, K. P. Kang, M. Jae Kang and S. K. Park, Chronic urate nephropathy with a disproportionated elevation in serum uric acid, *NDT Plus*, 2010, **3**, 320–321.

29 C. S. Chilappa, W. S. Aronow, D. Shapiro, K. Sperber, U. Patel and J. Y. Ash, Gout and hyperuricemia, *Compr. Ther.*, 2010, **36**, 3–13.

30 I. J. Di Fiore, G. Holloway and B. S. Coulson, Innate immune responses to rotavirus infection in macrophages depend on MAVS but involve neither the NLRP3 inflammasome nor JNK and p38 signaling pathways, *Virus Res.*, 2015, **208**, 89–97.

31 N. Liu, Z. Li, B. Meng, W. Bian, X. Li, S. Wang, X. Cao, Y. Song, M. Yang, Y. Wang, J. Tang and X. Yang, Accelerated Wound Healing Induced by a Novel Amphibian Peptide (OA-FF10), *Protein Pept. Lett.*, 2019, **26**, 261–270.

32 A. Haryono, D. A. A. Nugrahaningsih, D. C. R. Sari, M. M. Romi and N. Arfian, Reduction of Serum Uric Acid Associated with Attenuation of Renal Injury, Inflammation and Macrophages M1/M2 Ratio in Hyperuricemic Mice Model, *Kobe J. Med. Sci.*, 2018, **64**, E107–E114.

33 W. Bian, B. Meng, X. Li, S. Wang, X. Cao, N. Liu, M. Yang, J. Tang, Y. Wang and X. Yang, OA-GL21, a novel bioactive peptide from Odorrana andersonii, accelerated the healing of skin wounds, *Biosci. Rep.*, 2018, **38**, BSR20180215.

34 S. Yin, Y. Wang, N. Liu, M. Yang, Y. Hu, X. Li, Y. Fu, M. Luo, J. Sun and X. Yang, Potential skin protective effects after UVB irradiation afforded by an antioxidant peptide from Odorrana andersonii, *Biomed. Pharmacother.*, 2019, **120**, 109535.

35 B. Langmead and S. L. Salzberg, Fast gapped-read alignment with Bowtie 2, *Nat. Methods*, 2012, **9**, 357–359.

36 B. Li and C. N. Dewey, RSEM: accurate transcript quantification from RNA-Seq data with or without a reference genome, *BMC Bioinf.*, 2011, **12**, 323.

37 O. Trott and A. J. Olson, AutoDock Vina: improving the speed and accuracy of docking with a new scoring function, efficient optimization, and multithreading, *J. Comput. Chem.*, 2010, **31**, 455–461.

38 Y. Chen, C. Li, S. Duan, X. Yuan, J. Liang and S. Hou, Curcumin attenuates potassium oxonate-induced hyperuricemia and kidney inflammation in mice, *Biomed. Pharmacother.*, 2019, **118**, 109195.

39 C. Li, M. Chen, X. Li, M. Yang, Y. Wang and X. Yang, Purification and function of two analgesic and anti-inflammatory peptides from coelomic fluid of the earthworm, Eisenia foetida, *Peptides*, 2017, **89**, 71–81.

40 P. Parashar, I. Mazhar, J. Kanoujia, A. Yadav, P. Kumar, S. A. Saraf and S. Saha, Appraisal of anti-gout potential of colchicine-loaded chitosan nanoparticle gel in uric acid-induced gout animal model, *Arch. Physiol. Biochem.*, 2019, 1–11, DOI: 10.1080/13813455.2019.1702702.